Tetrahedron 66 (2010) 3930–3943

Contents lists available at ScienceDirect

Tetrahedron

journal homepage: www.elsevier.com/locate/tet

Synthesis and 'double click' density functionalization of 8-aza-7-deazaguanine DNA bearing branched side chains with terminal triple bonds

Frank Seela [a,b,*], Hai Xiong [a,b], Simone Budow [a]

[a] Laboratory of Bioorganic Chemistry and Chemical Biology, Center for Nanotechnology, Heisenbergstraße 11, 48149 Münster, Germany
[b] Laboratorium für Organische und Bioorganische Chemie, Institut für Chemie, Universität Osnabrück, Barbarastraße 7, 49069 Osnabrück, Germany

ARTICLE INFO

Article history:
Received 3 February 2010
Received in revised form 16 March 2010
Accepted 22 March 2010
Available online 27 March 2010

Keywords:
Pyrazolo[3,4-*d*]pyrimidine
Modified bases
Cycloaddition
Click reaction
DNA
Nucleosides
Oligonucleotides

ABSTRACT

The 7-[di(prop-2-ynl)amino]prop-1-ynyl derivative of 8-aza-7-deaza-2′-deoxyguanosine (**1**) was synthesized from 7-iodo-8-aza-7-deaza-2′-deoxyguanosine (**7**) by *Sonogashira* cross-coupling and converted into the phosphoramidite building block **10**. Oligonucleotides bearing branched side chains with terminal triple bonds were prepared by solid-phase synthesis containing single or multiple residues of **1** as 2′-deoxyguanosine surrogates. T_m measurements demonstrate that compound **1** has a positive effect on duplex stability, which is comparable to the stabilizing effect of the octa-1,7-diynylated non-branched nucleoside **2**. Nucleoside **1** and corresponding oligonucleotides were functionalized by the Cu(I)-mediated 1,3-dipolar cycloaddition 'double click' reaction with diverse ligands (AZT **3**, benzyl azide **4**, 11-azidoundecanol **5** and m-dPEG™$_4$-azide **6**). The conjugation reactions were carried out in solution and on solid support. Nucleoside **1** allowed 'double' functionalization of a single residue with two reporter groups. The 'double click' reaction proceeded smoothly even when two residues of nucleoside **1** were arranged in proximal positions. Hybridization with complementary strands led to a stable oligonucleotide duplex. Molecular modeling indicates that inspite of the crowded steric situation with four AZT ligands within closest proximal positions, all ligands are well accommodated in the major groove not disturbing the DNA helix.

1. Introduction

The copper(I)-catalyzed *Huisgen–Meldal-Sharpless* 1,3-dipolar cycloaddition of organic azides and alkynes (click reaction, CuAAC reaction) is widely used in synthetic chemistry,[1–3] bioconjugation [4,5] and materials science.[6–8] This cycloaddition is driven by the high energy content of the components (azides and alkynes) yielding less reactive 1,2,3-triazoles, which are highly stable to oxygen, light, and also in an aqueous environment.[1,2] In nucleic acid chemistry, the CuAAC reaction has been performed in solution [9–14], on solid support [15–19,20b], or on surfaces including biochip devices.[21–23] All four constituents of DNA or their analogs bearing terminal triple bonds were modified with different ligands at various position of single-stranded and duplex DNA.[13,20,24–29] Recently, protocols for double and multiple click reactions were developed as well as for sequential clicking.[30–32]

Among the variety of nucleobases, which are appropriate for DNA functionalization, the canonical pyrimidines modified at the 5-position were used for click reactions. 7-Deazapurines (pyrrolo[2,3-*d*]pyrimidines) were selected as purine surrogates, which were functionalized at position-7[25,26,32,33] (purine numbering is used in the results and discussion section). Our laboratory has reported on the synthesis and properties of oligonucleotides bearing tripropargylamine derivatives of 2′-deoxyuridine and 7-deaza-2′-deoxyguanosine introducing branched side chains with two terminal triple bonds in nucleosides and oligonucleotides.[30,32] Recently, it was demonstrated that, the functionalization of 8-aza-7-deazapurines (pyrazolo[3,4-*d*]pyrimidines) at the same position as pyrrolo[2,3-*d*]pyrimidines (position-7) shows advantages over that of the 7-deazapurines.[27]

We are now combining the favorable properties of pyrazolo[3,4-*d*]pyrimdines and branched side chains to click various ligands of different length and polarity to the DNA molecule. This leads to 'double click' conjugates with substituents of different spatial requirements within the major groove of duplex DNA. The 'double click' chemistry is performed on monomeric 8-aza-7-deaza-7-[(di(prop-2-ynl)amino)prop-1-ynyl]-2′-deoxyguanosine **1** and oligonucleotides with compound **1** as constituent (Fig. 1). Ligands, such as the non-polar and non-space demanding benzyl azide (**4**) as well as the more space demanding 3′-azido-2′,3′-dideoxythymidine (AZT; **3**) were chosen to prove the efficacy of 'double click' chemistry. The application of the 'double click' chemistry was extended to the field of nucleolipids and nucleoside–PEG/DNA–PEG conjugates using the long flexible lipohilic linker arms 11-azidoundecanol (**5**), or the m-dPEG™$_4$-azide **6** as ligands (Fig. 1). Both

* Corresponding author. Tel.: +49 251 53406 500; fax: +49 251 53406 857; e-mail addresses: frank.seela@uni-osnabrueck.de, seela@uni-muenster.de (F. Seela).
URL: http://www.seela.net

0040-4020/$ – see front matter © 2010 Elsevier Ltd. All rights reserved.
doi:10.1016/j.tet.2010.03.086

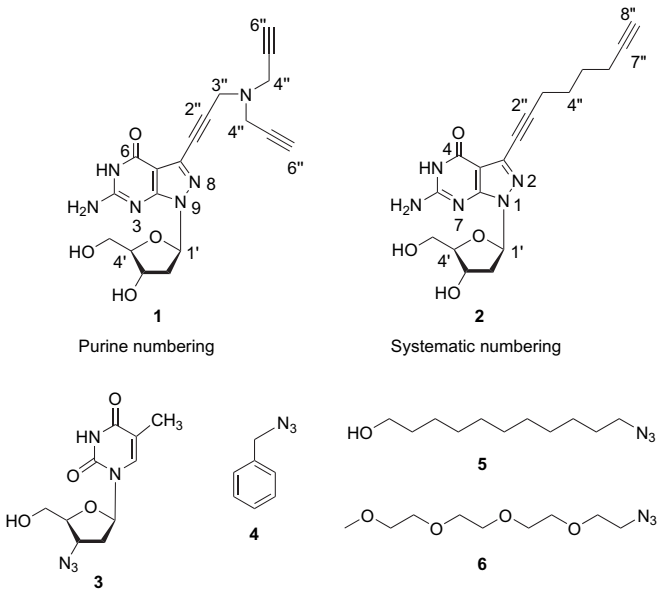

Figure 1. Structures of nucleosides and clickable ligands.

class of compounds attracted considerable interest as drug delivery systems or for applications in the field of material science and nanobiotechnology.[34–37] The 'double click' reactions were performed in solution and on solid support, and the influence of the various conjugates on the DNA duplex stability was studied.

Beside that, the branched side chain of nucleoside **1** containing two terminal triple bonds allows 'double' functionalization with two reporter groups per residue instead of 'mono' functionalization as it is the case for the earlier described compound **2**. In this context, high density functionalization of oligonucleotides is of current interest.[29,31,38–40] However, it is unknown whether the spatial demands of the branched side chains allow functionalization of multiple residues of **1** within a single-stranded oligonucleotide, especially if bulky residues are taken into account. To clarify this issue, separated as well as consecutive incorporations of nucleoside **1** into single-stranded oligonucleotides followed by post-functionalization were performed (Scheme 1).

2. Results and discussion

2.1. Nucleoside and phosphoramidite synthesis

Nucleoside **1** was synthesized from 7-iodo-7-deaza-8-aza-2′-deoxyguanosine (**7**) by *Sonogashira* cross-coupling.[41] The reaction was performed in dry DMF in the presence of Et_3N, $[Pd^0(PPh_3)_4]$ and CuI, with a 10-fold excess of tripropargylamine, leading to the exclusive formation of the mono-functionalized nucleoside **1** in 71% yield (Scheme 2). Compound **1** was protected at the 2-amino group with the isobutyryl residue affording the intermediate **8** in 84% yield. 4,4′-Dimethoxytritylation of the 5′-OH group and phosphitylation of the 3′-OH group under standard conditions furnished compounds **9** (86%) and **10** (83%), respectively. All compounds were characterized by elemental analyses, as well as by their ^1H and ^{13}C NMR spectra. The ^{13}C NMR chemical shifts are listed in Table 1, the

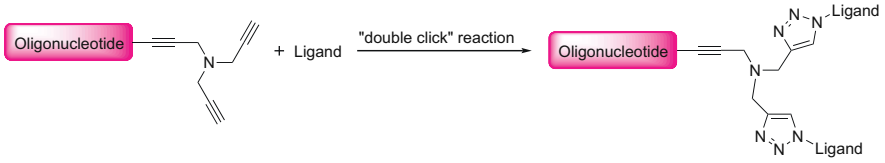

Scheme 1. Cu(I)-catalyzed 'double click' reaction using the alkyne-azide cycloaddition.

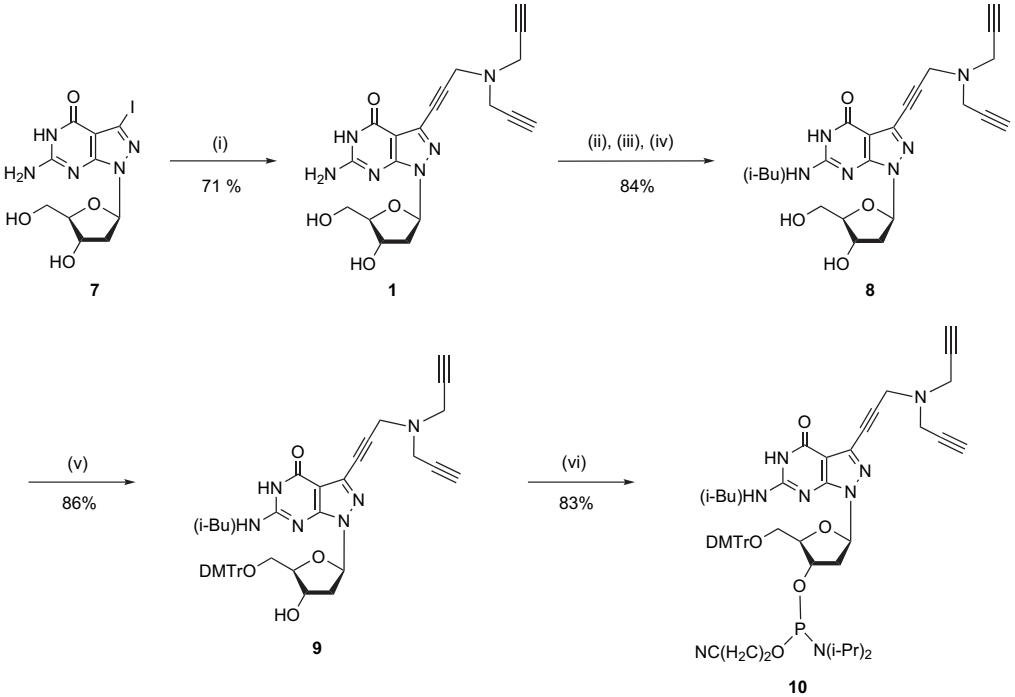

Scheme 2. Reagents and conditions. (i) tri(prop-2-ynyl)amine, $[Pd^0[P(Ph_3)_4]$, CuI, dry DMF, Et_3N, rt, 12 h; (ii) HMDS, rt, 3 h; (iii) anhydrous pyridine, *i*-Bu_2O, rt, overnight; (iv) MeOH, rt, 3 h; (v) 4,4′-dimethoxytriphenylmethyl chloride, anhydrous pyridine, $(i\text{-}Pr)_2EtN$, rt, 3 h; (vi) 2-cyanoethyl-*N*,*N*-diisopropylchlorophosphoramidite, anhydrous CH_2Cl_2, $(i\text{-}Pr)_2EtN$, rt, 30 min.

Table 1
^{13}C NMR chemical shifts of 8-aza-7-deaza-2′-deoxyguanosine derivatives and nucleoside conjugates **21**–**24**[a]

	C(2)[b] C(6)[c]	C(4)[b] C(7a)[c]	C(5)[b] C(3a)[c]	C(6)[b] C(4)[c]	C(7)[b] C(3)[c]	C≡C	CH_2	CH_3	C(1′)	C(2′)	C(3′)	C(4′)	C(5′)	Triazole
1	155.5[d]	155.3[d]	88.0	157.0[d]	129.5	100.4, 79.0, 77.3, 76.1	41.8, 41.2	—	83.2	37.7	70.9	87.6	62.4	—
8	152.8[d]	150.5[d]	89.0	155.1[d]	129.8	103.4, 78.9, 76.5, 76.1	41.8, 41.2	18.8	83.7	37.8	70.8	87.8	62.2	—
9	152.7[d]	150.5[d]	88.8	155.1[d]	135.6	103.6, 78.9, 76.7, 76.1	41.8, 41.2	18.8	84.0	38.0	70.4	85.6	64.0	—
21	155.6[d]	155.3[d]	88.2	157.2[d]	129.7	100.5, 77.7	52.8, 47.5, 41.7	—	83.2	37.7	71.0	87.6	62.4	143.7, 124.4
22	155.1[d]	154.8[d]	87.8	156.7[d]	129.3	100.0, 77.3	47.1, 41.2	11.8	83.4	37.2	70.4	87.1	61.9	143.3, 123.3
23	155.6[d]	155.3[d]	88.1	157.2[d]	129.7	100.4, 77.6	47.6, 41.6	—	83.2	37.7	70.9	87.5	62.4	143.3, 124.0
24	155.5[d]	155.3[d]	88.2	157.1[d]	129.7	100.4, 77.6	47.5, 41.5	58.0	83.2	37.7	70.9	87.5	62.4	143.2, 124.5

[a] Measured in [D_6]DMSO at 298 K.
[b] Purine numbering.
[c] Systematic numbering.
[d] Tentative.

Table 2
UV maxima and molar extinction coefficient (ε) of compound **1** and corresponding derivatives[a]

Cpd.	Wavelength λ_{max} [nm]	Mol. Ex. Coeff. (ε)	Cpd.	Wavelength λ_{max} [nm]	Mol. Ex. Coeff. (ε)
1	243	31,800	**21**	243	31,000
	280 (sh)	6500		285 (sh)	7000
$c^7z^8G_d$ (**2a**)[43]	254	14,200	**22**	244	31,000
				260	27,800
Octa $c^7z^8G_d$ (**2**)[27]	243	28,000	**23**	243	29,500
	280 (sh)	5400		286 (sh)	6200
8	243 (sh)	21,500	**24**	243	26,800
	251	23,800		286 (sh)	6700
	273	17,200			
9	235	34,200			
	250 (sh)	26,600			
	274	19,300			

[a] Measured in methanol.

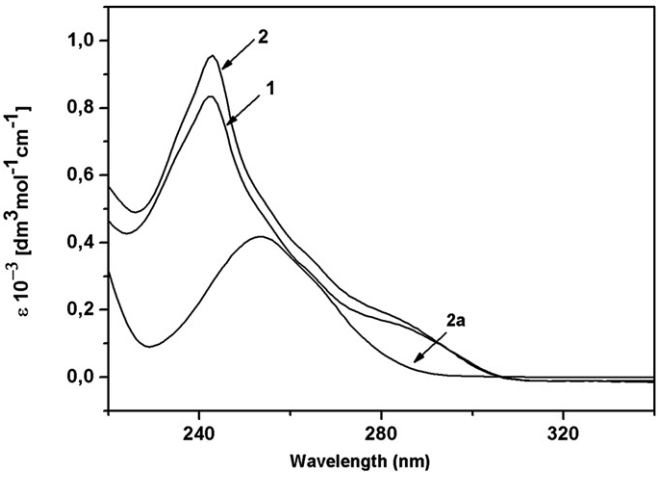

Figure 2. UV-spectra of 8-aza-7-deaza-2′-deoxyguanosine nucleosides **1** (c=0.0263 mmol L^{-1}), **2** (c=0.0358 mmol L^{-1}) and **2a** (c=0.0262 mmol L^{-1}) determined in methanol.

^1H–^{13}C-coupling constants were determined from ^1H–^{13}C gated-decoupled spectra (Table 5). The intact structure of the 7-[di(prop-2-ynyl)amino]prop-1-ynyl side chain was confirmed by ^{13}C NMR spectra showing two signals of the methylene groups (**1**: 41.8 and 41.2 ppm) and four signals for the triple bond carbons (**1**: 76.1, 77.3, 79.0, and 100.4 ppm; Table 1). Further confirmation of the structure was obtained by inverted signals of distortionless enhancement by polarization transfer (DEPT-135) spectra. From this, it was concluded that the triple bonds are not affected by the Pd-assisted *Sonogashira* cross-coupling (allene formation).[42]

2.2. Physical properties of nucleosides

All compounds were characterized by UV–vis spectroscopy performed in methanol (Table 2). The UV spectra of the tripropargylated 8-aza-7-deaza-2′-deoxyguanosine **1** is shown in Figure 2. For comparison, the UV spectra of the parent unmodified 8-aza-7-deaza-2′-deoxyguanosine (**2a**) as well as of the 7-octadiynylated compound **2** are shown (Fig. 2). The UV spectra and Table 2 indicate that, the 7-tripropargylamino and 7-octadiynyl side chain induce a hypsochromic shift (11 nm) compared to the non-functionalized 8-aza-7-deaza-2′-deoxyguanosine (**2a**). The UV spectra of compound **1** and **2** are almost similar indicating that the structure of their side chains has no influence on UV absorption.

The pK_a-values of nucleosides can strongly affect the base pairing properties and stabilities of oligonucleotide duplexes.[44] Although, the non-functionalized 8-aza-7-deaza-2′-deoxyguanosine (pK_a=9.3) exhibits a pK_a-value comparable to that of the canonical dG (pK_a=9.4) (Table 3), the influence of the tripropargylamino side chain is unknown. Consequently, the pK_a-value of compound **1** was measured UV-spectrophotometrically and compared with already existing data of 8-aza-7-deazapurine nucleosides. The representative titration profile of compound **1** is shown in Table 3 (for pH-dependent UV-spectra, see Supplementary data Fig. S1). The 7-tripropargylamino substituent has almost no influence on the pK_a-value (**1**: pK_a=9.2), which is consistent with observations made for propynylated or octadiynylated 8-aza-7-deaza-2′-deoxyguanosine nucleosides.

2.3. Synthesis and duplex stability of oligonucleotides containing nucleoside 1

In order to evaluate the influence of branched bulky linker arms with terminal triple bonds on the DNA duplex stability, a series of oligonucleotides were prepared by solid-phase synthesis using the phosphoramidite **10** as well as standard phosphoramidites. The

Table 3
pK_a-values of selected nucleosides[a] and UV spectrum of nucleoside **1** as a function of pH values

Compound	Wavelength[b] [nm]	pK_a[c]	Ref.
dG		9.4	45
$c^7z^8G_d$ (**2a**)	248	9.3	43
Prop $c^7z^8G_d$ (**2b**)	245	8.9	27
Octa $c^7z^8G_d$ (**2**)	246	9.0	27
TriPA $c^7z^8G_d$ (**1**)	246	9.2	

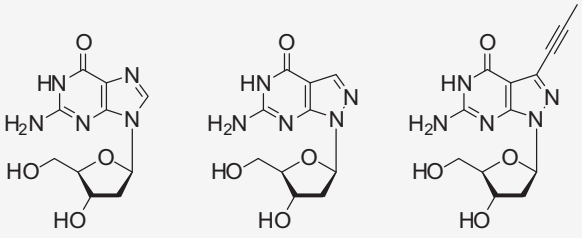

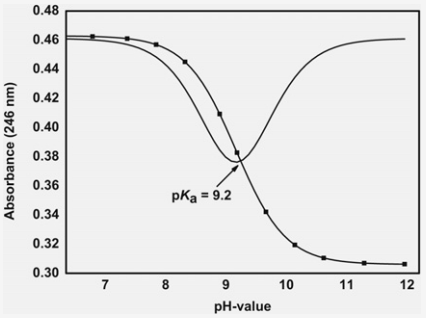

UV spectroscopic change of 7-tripropargylamino-8-aza-7-deaza-2′-deoxyguanosine (**1**) measured in 0.1 M sodium phosphate buffer monitored at 246 nm with a concentration of 1.66×10^4 μM at various pH values.

[a] Measured in phosphate buffer (0.1 M NaH_2PO_4) from pH 2 to pH 12.5.
[b] Wavelength of measurements as indicated.
[c] Deprotonation.

synthesis was performed in a 1 μmol scale. The coupling yields were always higher than 95%. Deprotection of the oligomers was performed in aqueous NH_3 (25%) at 60 °C for 14 h. The oligonucleotides were purified before and after detritylation by reversed-phase HPLC. The homogeneity of the oligonucleotides was confirmed by HPLC analysis (see Supplementary data, Fig. S3) and their molecular weights were determined by MALDI-TOF mass spectrometry (Table 7). Single and multiple incorporations of **1**, replacing dG-residues within various positions of the reference duplex 5′-d(TAG GTC AAT ACT) (**11**) and 3′-d(ATC CAG TTA TGA) (**12**) were performed and the duplex stability of the modified duplexes was investigated by T_m measurements. These data are compared with oligonucleotide duplexes containing the non-branched octa-1,7-diynyl nucleoside **2**. The T_m values listed in Table 4 were measured under high salt (1 M NaCl) conditions at pH 7.2 and pH 8.5 with a 2 μM concentration of the single-strands. Data in parentheses are T_m values measured at 5 μM single-strand concentration.

From Table 4 the following conclusions can be drawn: (i) Replacement of one 2′-deoxyguanosine residue by nucleoside **1** in the center of the duplex (**11**·**14**) does not change the T_m value while a modification at the 5′-terminus increases its stability significantly (**11**·**13**: ΔT_m=+5 °C) compared to reference duplex (**11**·**12**). (ii) Multiple incorporations have a positive effect on the duplex stability. (iii) Modifications at the same positions by the non-branched nucleoside **2** have a similar effect as those with branched side chains (**1**). (iv) A concentration increase from 2 μM to 5 μM leads to a T_m increase of about 1 °C. (v) An increased pH value decreases the T_m value for duplexes containing the branched linker (**1**) or the non-branched nucleosides (**2**).

2.4. Functionalization of nucleoside 1 with diverse ligands by the ‘double click’ reaction

Hybrid molecules composed of two or more chemical subunits are ubiquitous, both in nature as well as in synthetic chemistry.[34] The CuAAC reaction is a versatile method to connect functionalized precursors with appropriate ligands to obtain hybrid molecules with various characteristics. In this manuscript, the branched 7-tripropargylamine-8-aza-7-deaza-2′-deoxyguanosine (**1**) and oligonucleotides containing one or two residues of **1** were used as precursors. The efficacy and versatility of the ‘double click’ reaction was now evaluated employing ligand molecules of different polarity and spatial requirements. Among the selected ligands, the aromatic benzyl azide (**4**) is the most non-polar molecule with little steric demand. The antivirally active 3′-azido-2′,3′-dideoxythymidine (AZT; **3**) can be considered as a polar and bulky ligand with enhanced spatial requirements compared to **4**. The applicability of the ‘double click’ reaction was also probed for the construction of nucleolipids, which are composed of a lipophilic moiety and a nucleobase, nucleoside, nucleotide or oligonucleotide unit.[34,46] In this study, the long and flexible linker 11-azidoundecanol (**5**) was chosen as lipophilic moiety. Another class of hybrid molecules being accessible by the ‘double click’ reaction are the nucleoside–PEG and DNA–PEG conjugates; herein being exemplified for the hydrophilic ligand 1-azido-polyethylenglycol **6** (m-dPEG™$_4$-azide). Both, nucleolipids and DNA–PEG conjugates are promising candidates for oligonucleotide drug delivery systems.[34–37] Due to the favorable properties, these classes of molecules have also attracted considerable interest for applications in material science and nanobiotechnology.[34,47]

In a first series of experiments, the ‘double click’ reaction was performed on the monomeric nucleoside **1** containing two terminal triple bonds. The ‘double click’ reaction using benzyl azide (**4**) as ligand was carried out in the presence of $CuSO_4$ and sodium ascorbate in a 3:1:1 mixture of THF/*t*-BuOH/H_2O. A 2.4-fold excess of azide and a reaction time of 16 h was necessary to complete the reaction and to obtain the ‘double click’ conjugate **21** in 78% yield; no mono-functionalized derivative was detected (Scheme 3). The bis-functionalization of the tripropargylamino side chain was also performed with AZT (**3**) bearing an azido group in the 3′-position. Spatial crowdedness caused by the two AZT residues within the ‘double click’ conjugate **22** is strongly enhanced compared to the spatial situation of conjugate **21** carrying two benzyl ligands. Nevertheless, only the bis-functionalized adduct **22** was obtained; however the yield was significant lower (54% yield). Here, the synthesis was performed in a 3:1 mixture of THF/H_2O using a 2.4-fold excess of AZT (**3**) and a reaction time of 12 h with the same catalyst as described above (Scheme 3). The same solvent system was employed for the conjugation of nucleoside **1** and the long chain ligands **5** and **6**. A 2-fold excess of the respective ligand and a reaction time of 16 h in the presence of $CuSO_4$ and sodium ascorbate afforded the ‘double click’ conjugates **23** (54%) and **24** (39%) in moderate yield.

The structures of the ‘double click’ products **21**–**24** were confirmed by their ^{1}H, ^{13}C, ^{1}H–^{13}C-gated-decoupled as well as DEPT-135 NMR spectra (Tables 1, 5 and Experimental part). Due to the formation of the 1,2,3-triazole ring, the signals of the acetylenic protons of **1** disappeared (δ_H=3.25 ppm). Signals indicating the new methylidene protons (δ_H=3.8–3.9 ppm) and the triazole hydrogen H–C5 (δ_H=8.1–8.3 ppm) were identified for the ‘double click’ conjugates **21**–**24**. Furthermore, ^{13}C NMR spectra show the absence of the two terminal C≡C carbon atom signals while two new double bond carbon signals of the 1,2,3-triazole moiety are appearing. As indicated in Table 1, they are located around 143 ppm (quaternary C-atom) and 123 to 124 ppm (triazole-C5) (**21**: δ=143.8, 124.4 ppm; **22**: δ=143.3, 124.3 ppm; **23**: δ=143.3, 124.0 ppm; **24**: δ=143.2, 124.5 ppm). In all cases the ^1J(C, H) coupling constant for the triazole-C5, H–C5 obtained from ^{1}H–^{13}C-gated-decoupled NMR spectroscopy is about 196 Hz (Table 5).

Table 4
T_m-values of oligonucleotide duplexes containing the branched nucleoside **1** or the non-branched derivative **2**

Duplexes	T_m[a] [°C] pH=7.2	ΔT_m[b] [°C]	T_m[c] [°C] pH=8.5	ΔT_m[b] [°C]
5′-d(TAG GTC AAT ACT) (**11**) 3′-d(ATC CAG TTA TGA) (**12**)	49 (50)	—	46	—
5′-d(TAG GTC AAT ACT) (**11**) 3′-d(ATC CAG TTA T**1**A) (**13**)	54 (55)	+5	51	+5
5′-d(TAG GTC AAT ACT) (**11**) 3′-d(ATC CA**1** TTA TGA) (**14**)	49 (51)	0	46	0
5′-d(TA**1** **1**TC AAT ACT) (**15**) 3′-d(ATC CAG TTA TGA) (**12**)	52 (54)	+1.5	51	+2.5
5′-d(TAG GTC AAT ACT) (**11**) 3′-d(ATC CA**1** TTA T**1**A) (**16**)	52 (53)	+1.5	49	+1.5
5′-d(TAG GTC AAT ACT) (**11**) 3′-d(ATC CAG TTA T**2**A) (**17**)	52	+3	49	+3
5′-d(TAG GTC AAT ACT) (**11**) 3′-d(ATC CA**2** TTA TGA) (**18**)	49	0	46	0
5′-d(TA**2** **2**TC AAT ACT) (**19**) 3′-d(ATC CAG TTA TGA) (**12**)	53	+2	50	+2
5′-d(TAG GTC AAT ACT) (**11**) 3′-d(ATC CA**2** TTA T**2**A) (**20**)	51	+1	49	+1.5

[a] Measured at 260 nm in 1 M NaCl, 100 mM $MgCl_2$, and 60 mM Na-cacodylate (pH 7.2) with 2 μM+2 μM single-strand concentration. Data given in parenthesis refer to a 5 μM+5 μM single-strand concentration.
[b] Refers to the contribution of the modified residues divided by the number of replacements.
[c] Measured at 260 nm in 1 M NaCl, 100 mM $MgCl_2$, and 60 mM Na-cacodylate (pH 8.5) with 2 μM+2 μM single-strand concentration.

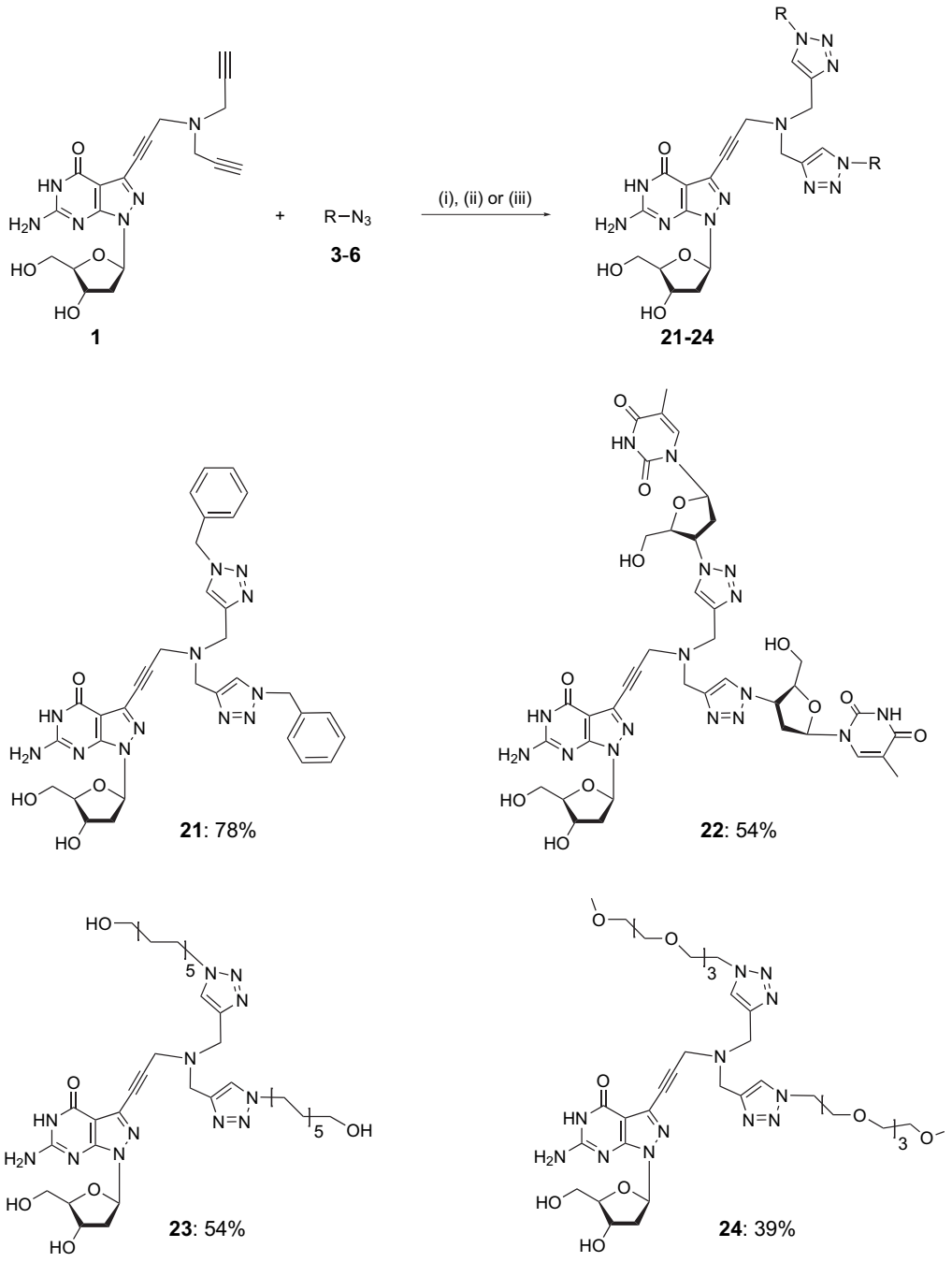

Scheme 3. Synthesis of 1,2,3-triazolyl nucleoside conjugates **21**–**24**. (i) $CuSO_4$, sodium ascorbate, THF/*t*-BuOH/H_2O, 16 h, rt; (ii) $CuSO_4$, sodium ascorbate, THF/H_2O, 12 h, rt; (iii) $CuSO_4$, sodium ascorbate, THF/H_2O, 16 h, rt.

2.5. Density functionalization of oligonucleotides by the 'double click' reaction

High density functionalization of DNA is encountered with various difficulties. Most of the activated ligands are not selective and reactive enough. Excess reagent has to be used to complete the reaction, which has to be removed afterward. The situation becomes even more problematic when the ligands have to be incorporated into proximal positions. The click reaction was used to overcome these difficulties.[24] However, only a single reporter group was introduced per modified residue. Contrary, 'double click' chemistry employing tripropargylated nucleosides, such as **1** with two terminal triple bonds, allows 'double' functionalization with two reporter groups per residue instead of 'mono' functionalization. Recently, the 'double click' reaction was performed on single-stranded oligonucleotides containing tripropargylated 2′-deoxyuridine or 7-deaza-2′-deoxyadenosine residues using AZT,[30] 3-azido-7-hydroxycoumarin[30] or 1-azidomethyl pyrene[32] as reporter groups. However, hitherto, functionalization was carried out only on oligonucleotides containing a single tripropargylated residue.[30,32]

To prove the versatility of nucleoside **1** as constituent of oligonucleotides in post-labeling, the four ligands **3**–**6** employed for the 'double click' reaction on monomeric level were used first for oligonucleotide functionalization. The conjugation reaction was carried out in solution with **3**–**6**, and alternatively with **3**, **4** on solid support (CPG) bounded oligonucleotides containing one modification site. Up to now, it has not been shown that the steric

Table 5
Coupling constants *J*(C,H) [Hz] of click conjugates **21**–**24**[a,b]

	Coupling	*J* [Hz]				
		1	**21**	**22**	**23**	**24**
C5	^{3}J(C5, H–C1′)	8.7	8.1	7.9	8.1	7.9
C1″≡	^{3}J(C1″, H–C3″)	—	3.1	—	—	—
C2″≡	^{2}J(C2″, H–C3″)	4.2	4.3	3.9	4.6	4.2
C3″ or C4″ [c]	^{1}J(C3″, H–C3″) or ^{1}J(C4″, H–C4″)	136 or 142	136, n.d.	135, n.d.	134, n.d.	142, n.d.
C5″	^{2}J(C5″, H–C6″),	50	—	—	—	—
	^{2}J(C5″, H–C4″)	8.3	—	—	—	—
C6″	^{1}J(C6″, H–C6″),	250	—	—	—	—
	^{3}J(C6″, H–C4′)	3.8	—	—	—	—
Triazole-C5	^{1}J(triazole-C5, H–C5)	—	196	196	195	196
C1′	^{1}J(C1′, H–C1′)	165	161	169	165	164
C2′	^{1}J(C2′, H–C2′)	134	134	133	134	133
C3′	^{1}J(C3′, H–C3′)	150	149	145	148	150
C4′	^{1}J(C4′, H–C4′)	149	147	148	148	150
C5′	^{1}J(C5′, H–C5′)	140	141	141	139	141

[a] Measured in [D_6]DMSO at 298 K.
[b] Purine numbering.
[c] Tentative. n.d. not detected.

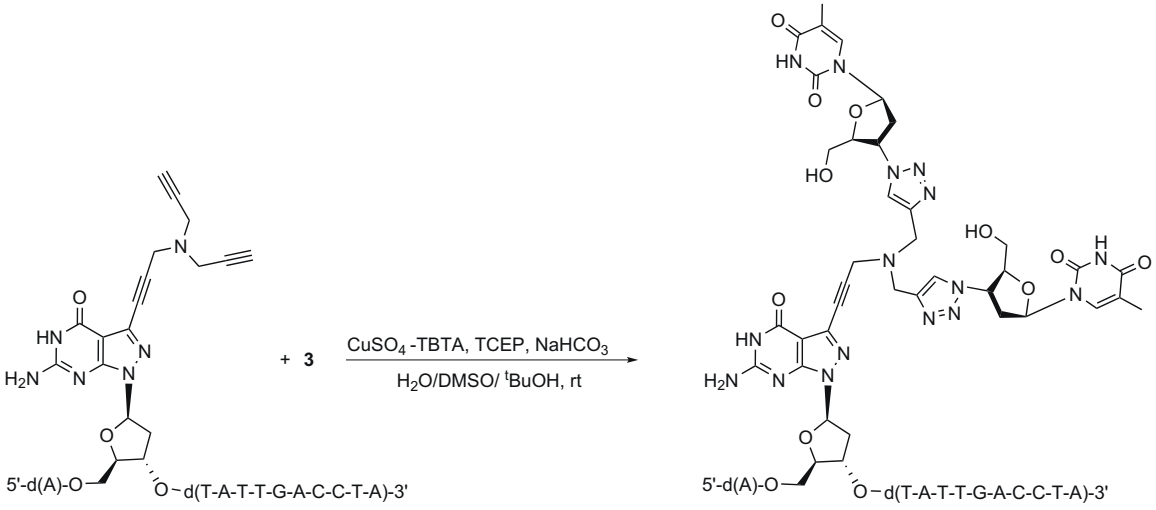

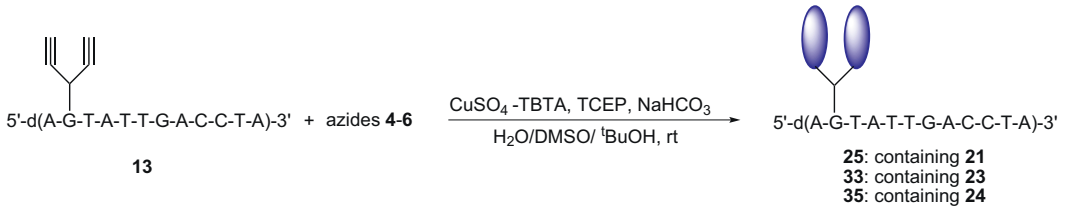

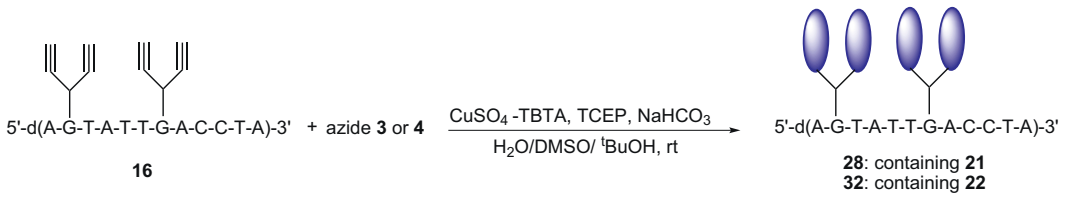

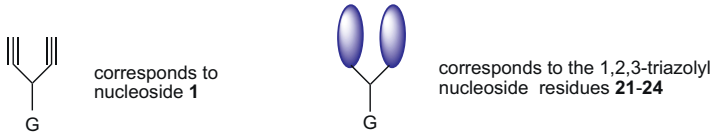

Scheme 4. *Huisgen–Meldal-Sharpless* [2+3] cycloaddition of oligonucleotides **13** and **16** incorporating nucleoside **1** with azides (AZT **3**, benzyl azide **4**, 11-azidoundecanol **5**, m-dPEG™$_4$-azide **6**).

Table 6
T_m-values of oligonucleotide duplexes containing the 'double click' conjugates **21**–**24**

Duplexes	T_m[a] [°C]	ΔT_m[b] [°C]
5′-d(TAG GTC AAT ACT) (**11**) 3′-d(ATC CAG TTA TGA) (**12**)	49	—
5′-d(TAG GTC AAT ACT) (**11**) 3′-d(ATC CAG TTA T**21**A) (**25**)	51	+2
5′-d(TAG GTC AAT ACT) (**11**) 3′-d(ATC CA**21** TTA TGA) (**26**)	47	−2
5′-d(TA**21** **21**TC AAT ACT) (**27**) 3′-d(ATC CAG TTA TGA) (**12**)	47	−1
5′-d(TAG GTC AAT ACT) (**11**) 3′-d(ATC CA**21** TTA T**21**A) (**28**)	42	−3.5
5′-d(TAG GTC AAT ACT) (**11**) 3′-d(ATC CAG TTA T**22**A) (**29**)	49	0
5′-d(TAG GTC AAT ACT) (**11**) 3′-d(ATC CA**22** TTA TGA) (**30**)	48	−1
5′-d(TA**22** **22**TC AAT ACT) (**31**) 3′-d(ATC CAG TTA TGA) (**12**)	49	0
5′-d(TAG GTC AAT ACT) (**11**) 3′-d(ATC CA**22** TTA T**22**A) (**32**)	46	−1.5
5′-d(TAG GTC AAT ACT) (**11**) 3′-d(ATC CAG TTA T**23**A) (**33**)	49	0
5′-d(TAG GTC AAT ACT) (**11**) 3′-d(ATC CA**23** TTA TGA) (**34**)	41	−8
5′-d(TAG GTC AAT ACT) (**11**) 3′-d(ATC CAG TTA T**24**A) (**35**)	49	0
5′-d(TAG GTC AAT ACT) (**11**) 3′-d(ATC CA**24** TTA TGA) (**36**)	43	−6

[a] Measured at 260 nm in 1 M NaCl, 100 mM $MgCl_2$, and 60 mM Na-cacodylate (pH 7.2) with 2 μM+2 μM single-strand concentration.
[b] Refers to the contribution of the modified residues divided by the number of replacements.

demands of the branched side chain allow density functionalization. Especially, side by side arranged residues cause a particular crowded situation upon functionalization. To probe density functionalization, the 'double' CuAAC reaction was also performed on oligonucleotides incorporating two residues of compound **1** with the ligands **3** and **4**. Two alternative protocols have been used for the 'double click' reaction; functionalization employing (i) oligonucleotides in solution or (ii) solid-phase bounded oligonucleotides. At first, the 'double click' reaction was performed on the oligonucleotides 5′-d(A**1**T ATT GAC CTA) (**13**) and 5′-d(AGT ATT **1**AC CTA) (**14**), each containing one 7-tripropargylamine-8-aza-7-deaza-2′-deoxyguanosine residue. The ligands **3**–**6** were subjected to 'double click' reactions with both oligonucleotides. The reaction was carried out in aqueous solution (H_2O/DMSO/*t*-BuOH) employing a premixed 1:1 complex of $CuSO_4$·TBTA (tris(benzyltriazoylmethyl)amine), TCEP (tris(carboxyethyl)phosphine) and $NaHCO_3$ (Scheme 4). $NaHCO_3$ was essential to complete the reaction within 12 h. Different concentrations of the individual azides and reagents were employed for functionalization (for details see the Experimental section), yielding the oligonucleotide conjugates **25**, **26**, **29**, **30**, **33**–**36** (see Table 6). They were purified by reversed-phase HPLC (RP-18 column) and characterized by HPLC chromatography (see Supplementary data, Figs. S4–6) as well as by MALDI-TOF mass spectrometry (Table 7).

Next, density functionalization was probed using the oligonucleotides 5′-d(TA**1** **1**TC AAT ACT) (**15**) and 5′-d(A**1**T ATT **1**AC CTA) (**16**). The modification sites are arranged consecutively (→**15**) or are separated by four nucleosides (→**16**). However, in both cases, functionalization introduces four reporter groups into one 12-*mer* single-stranded oligonucleotide. The 'double click' reaction was carried out as described above employing benzyl azide (**4**) and AZT (**3**) as ligands (Scheme 4 and for details see the Experimental section). In all cases, the reactions proceeded smoothly and no mono-functionalized oligonucleotide was observed during HPLC chromatography. The excellent Cu(I) ligand-binding properties of tripropargylamine derivatives together with the formation of triazole units might drive the reaction toward difunctionalized conjugates. HPLC purification afforded the oligonucleotide conjugates **27**, **28** and **31**, **32** (see Table 6). Consequently, the tripropargylated nucleoside **1** can be considered as an ideal 'clickable' functionalization site as even reporter groups with severe spatial requirement such as AZT (**3**) can be introduced in consecutive position, e.g., oligonucleotide conjugate **27**. Oligonucleotide conjugates **27**, **28** and **31**, **32** were characterized by HPLC RP-18 chromatography (see Supplementary data, Figs. S4, S5) and their correct masses were confirmed by mass spectrometry (Table 7).

Alternatively, the 'double click' reaction was carried out on solid support (CPG) bounded oligonucleotides employing AZT (**3**) and benzyl azide (**4**) as ligands. For this purpose, the CPG-bound 12-*mer* oligonucleotides 5′-d((5′-*O*-$(MeO)_2$Tr)A**1**T ATT GAC CTA) (**37**) and 5′-d((5′-*O*-$(MeO)_2$Tr)A**1**T ATT **1**AC CTA) (**42**) were synthesized by solid-phase synthesis using the regular phosphoramidites and the modified building block **10**. The $(MeO)_2$Tr protecting group was preserved on the CPG-bound oligonucleotides **37** and **42**, and the 'double click' reaction was performed with AZT (**3**) in aqueous solution (H_2O/DMSO/*t*-BuOH, 4:3:1) and the above mentioned reagents (see Experimental section) to give the crude functionalized oligomers **38** and **43** (Scheme 5). To remove excess AZT (**3**) and the reagents present in the reaction mixture, the crude matrix-bound **38** and **43** were washed with MeOH/H_2O (1:1). Thereafter, the oligonucleotides were cleaved from the solid support using standard deprotection conditions (25% aqueous NH_3 solution, 60 °C, 14 h). During this procedure, the base-labile protecting groups were also removed. Purification of the obtained 5′-*O*-dimethoxytrityl oligonucleotide conjugates **40** and **45** was performed by reversed-phase HPLC (RP-18 column). The $(MeO)_2$Tr protecting group was removed (2.5% $Cl_2CHCOOH$ in CH_2Cl_2) followed by further purification yielding oligonucleotides **29** and **32** (see Experimental section). The structures of the ligation products were confirmed by MALDI-TOF mass spectrometry. Similarly, the 'double click' reaction was performed with benzyl azide (**4**) and the CPG-bound oligonucleotides **37** and **42** yielding

Table 7
Molecular mass $[M-1]^-$ of selected oligonucleotides determined by MALDI-TOF mass spectrometry[a]

Oligonucleotides	$[M-1]^-$		Oligonucleotides	$[M-1]^-$	
	(calcd)	(Found)		(calcd)	(Found)
5′-d(A**1**T ATT GAC CTA) (**13**)	3772.6	3772.6	5′-d(AGT ATT **22**AC CTA) (**30**)	4307.0	4036.8
5′-d(AGT ATT **1**AC CTA) (**14**)	3772.6	3772.0	5′-d(AGT ATT **21**AC CTA) (**26**)	4038.9	4038.2
5′-d(TA**1** **1**TC AAT ACT) (**15**)	3901.7	3900.9	5′-d(AGT ATT **23**AC CTA) (**34**)	4199.2	4198.6
5′-d(A**1**T ATT **1**AC CTA) (**16**)	3901.7	3902.3	5′-d(AGT ATT **24**AC CTA) (**36**)	4239.1	4239.2
5′-d(A**2**T ATT **2**AC CTA) (**20**)	3851.7	3851.8	5′-d(TA**22** **22**TC AA TACT) (**31**)	4970.7	4971.3
5′-d(A**22**T ATT GAC CTA) (**29**)	4307.0	4306.5	5′-d(TA**21** **21**TC AAT ACT) (**27**)	4434.3	4433.7
5′-d(A**21**T ATT GAC CTA) (**25**)	4038.9	4038.8	5′-d(A**22**T ATT **22**AC CTA) (**32**)	4970.7	4970.6
5′-d(A**23**T ATT GAC CTA) (**33**)	4199.2	4199.0	5′-d(A**21**T ATT **21**AC CTA) (**28**)	4434.3	4435.3
5′-d(A**24**T ATT GAC CTA) (**35**)	4239.1	4238.1			

[a] Determined as $[M-1]^-$ in the linear negative mode.

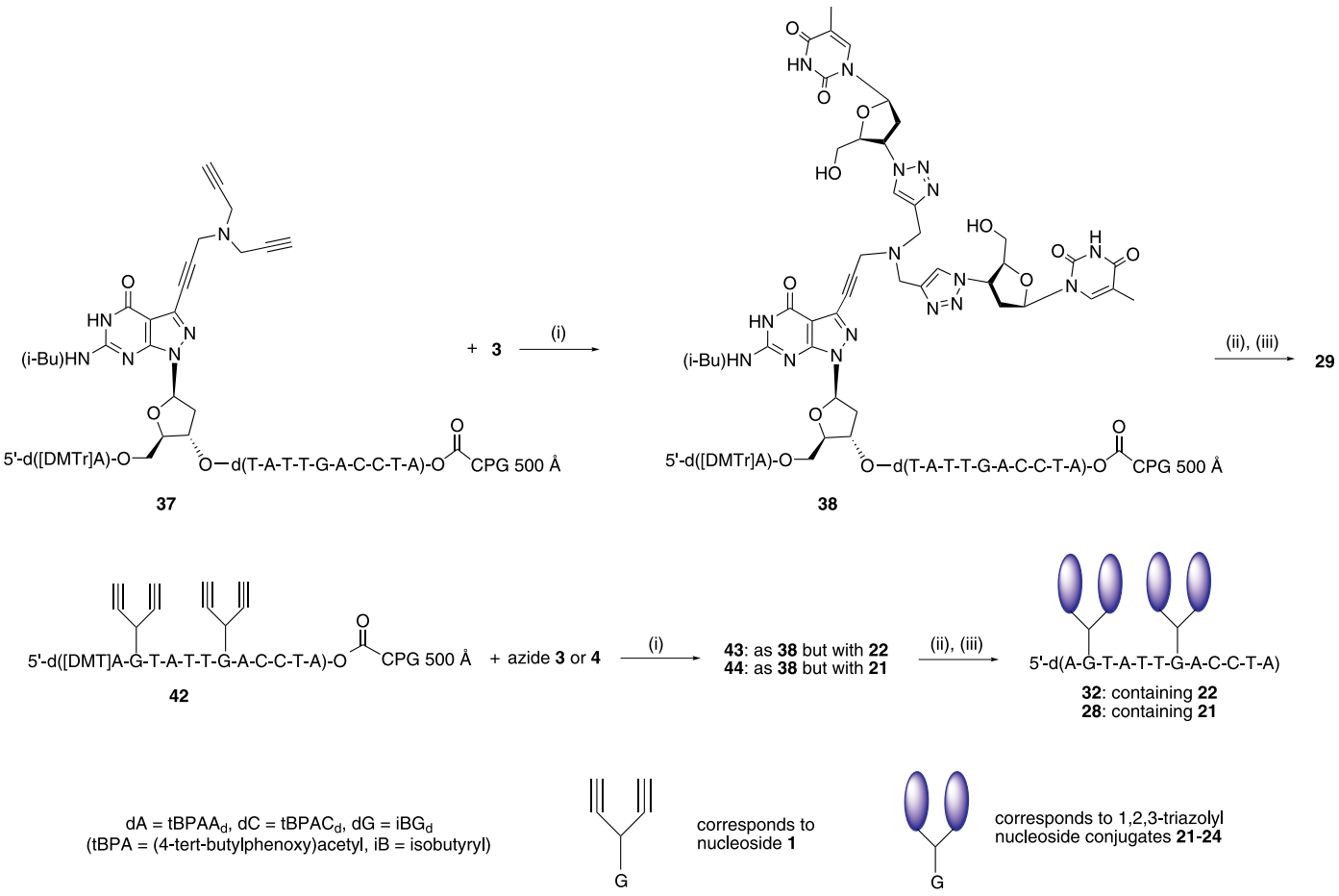

Scheme 5. Functionalization of tripropargylamine oligonucleotides with AZT (**3**) or benzyl azide (**4**) on solid support. The phosphates in solid-support-bound oligonucleotides **37** and **42** are *O-cyanoethyl* protected. Reagents and conditions. (i) $CuSO_4$-TBTA, TCEP, $NaHCO_3$, H_2O/DMSO/t-BuOH, rt; (ii) aq. NH_3, 60°C, 14 h; (iii) 2.5% DCA/CH_2Cl_2.

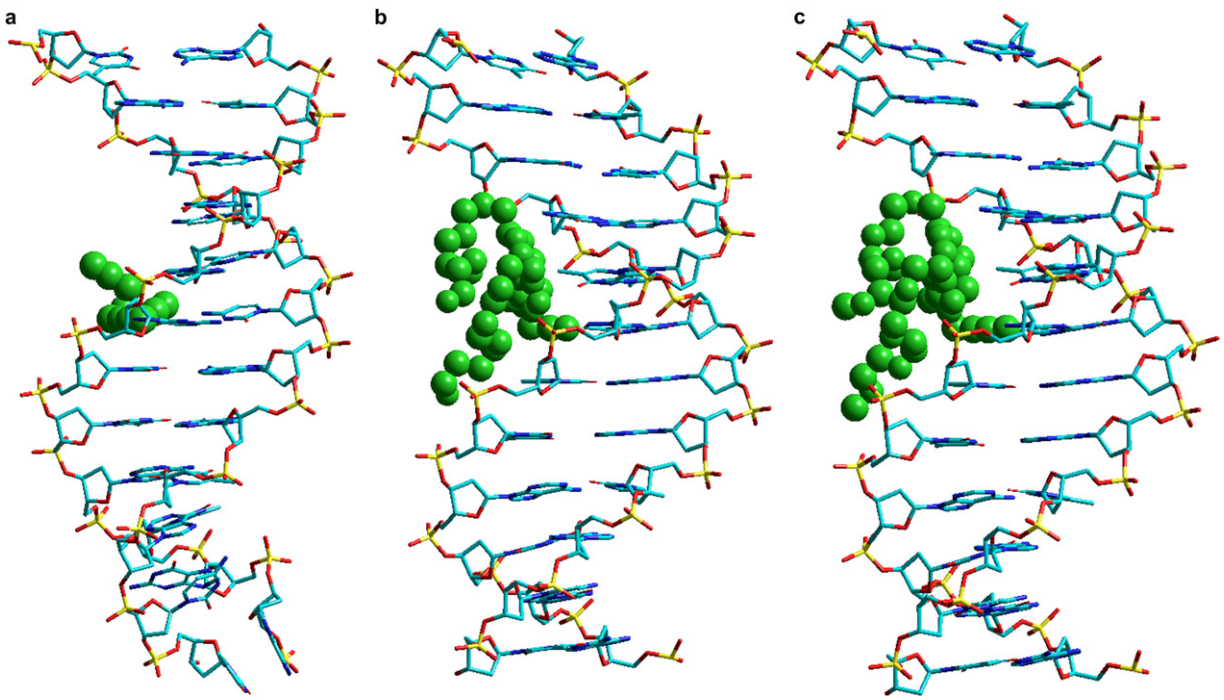

Figure 3. Molecular models of (a) duplex 5′-d(TAG GTC AAT ACT) (**11**) · 3′-d(ATC CA**1** TTA TGA) (**14**), (b) duplex 5′-d(TAG GTC AAT ACT) (**11**) · 3′-d(ATC CA**23** TTA TGA) (**34**) and (c) duplex 5′-d(TAG GTC AAT ACT) (**11**) · 3′-d(ATC CA**24** TTA TGA) (**36**). The models were constructed using Hyperchem 8.0 and energy minimized using AMBER calculations. The modification sites are presented as green space filling balls.

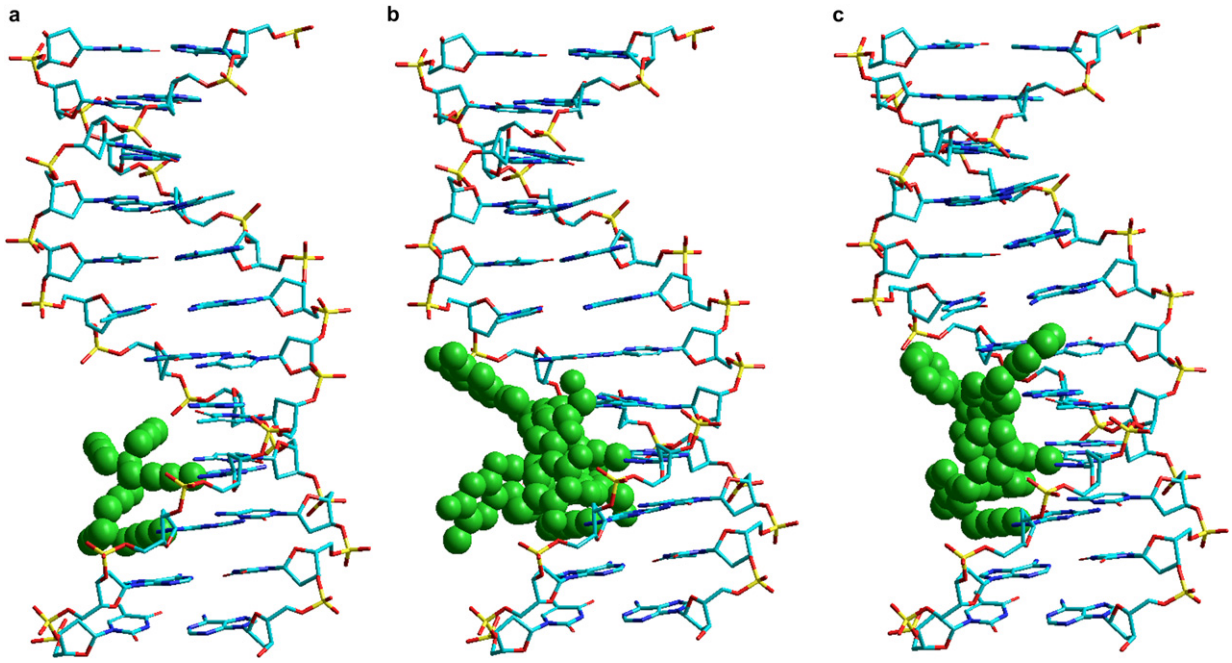

Figure 4. Molecular models of (a) duplex 5′-d(TA**1** **1**TC AAT ACT) (**15**) · 3′-d(ATC CAG TTA TGA) (**12**), (b) duplex 5′-d(TA**22** **22**TC AAT ACT) (**31**) · 3′-d(ATC CAG TTA TGA) (**12**) and (c) duplex 5′-d(TA**21** **21**TC AAT ACT) (**27**) · 3′-d(ATC CAG TTA TGA) (**12**). The models were constructed using Hyperchem 8.0 and energy minimized using AMBER calculations. The modification sites are presented as green space filling balls.

oligonucleotides **25** and **28** (see Experimental section). This method allows easy removal of unreacted starting material and reagents facilitating purification of the click products. Our results show that this approach is suitable for introducing non-polar reporter groups (benzyl azide, **4**) as well as for space demanding ligands (AZT, **3**). High density functionalization of oligonucleotides is possible as demonstrated for oligomers **28** and **32**, each containing four reporter groups per one 12-*mer* single-strand.

2.6. Duplex stability of oligonucleotide 'double click' conjugates

Next, the influence of the ligands **3**–**6** introduced by the 'double click' reaction on duplex stability was evaluated (Table 6). T_m measurements were carried out in high salt buffer (1 M NaCl) using 2 μM single-strand concentration. Again, the duplex 5′-d(TAG GTC AAT ACT) (**11**) · 3′-d(ATC CAG TTA TGA) (**12**) was used as reference. The replacement of one dG residue by the 'double click' conjugates **22**, **23** or **24** at the peripheral of the standard duplex had no influence on the duplex stability (ΔT_m=0 °C). Only the introduction of the benzyl azide conjugate **21** at this position led to a stabilization (ΔT_m=+2 °C). On the contrary, replacements within a central position of the duplex cause destabilization. In the case of the long chain linker conjugates **23** and **24**, the T_m values decreased significantly (ΔT_m=−8 °C for **23** and ΔT_m=−6 °C for **24**). This result was unexpected as PEG–DNA is considered for drug delivery systems. However, our result points to the fact that the PEG modification site has to be carefully selected to avoid destabilizing effects.

Next, incorporation of multiple residues of **21** and **22** were investigated, which were arranged consecutively or were separated by four base pairs. Surprisingly, the consecutive incorporation of the AZT clicked conjugate **22** bringing four space demanding residues into close proximity (duplex **31**·**12**) has no negative effect on duplex stability (ΔT_m=0 °C) indicating that all four residues are well accommodated into the major groove of the duplex. For illustration of the steric situation see also Figure 4 in the next section. Separation of the modified residues destabilizes the duplex **11**·**32** by −3 °C compared to the reference duplex **11**·**12**. For duplexes **27**·**12** and **11**·**28**, incorporating the 'double click' conjugate **21**, a similar tendency can be observed; however with a more pronounced destabilization of −2 °C for **27**·**12** (consecutive modification sites) and −7 °C for **11**·**28** (separated modification sites).

2.7. Molecular dynamics simulations

Molecular dynamics simulations using Amber MM+ force field (Hyperchem 8.0; Hypercube Inc., Gainesville, FL, USA, 2001) were performed on the 12-*mer* duplexes **11**·**14**, **11**·**34**, and **11**·**36** containing one modification site within the center of the duplex (Fig. 3) as well as **15**·**12**, **27**·**12**, and **31**·**12** containing two consecutive modification sites (Fig. 4). The energy minimized molecular structures are built as B-type DNA. Figure 3a displays a duplex in which a central dG residue is displaced by the 7-tripropargylated derivative of 8-aza-7-deaza-2′-deoxyguanosine (**1**). In Figure 3b,c, this position is modified by the conjugate derived from the 'double click' reaction with 11-azidoundecanol (**23**) and the m-dPEG™$_4$-azide (**24**). In both cases, the long chains are well accommodated in the major groove of DNA and seem not to interfere with the DNA helix. Moreover, the triazole rings are not involved into stacking interactions with the base pairs.

Figure 4 illustrates the steric situation for consecutive modification sites. The four linker arms of duplex **15**·**12** are situated in the major groove pointing away from each (Fig. 4a). Functionalization with AZT (**3**) or benzyl azide (**4**) causes a crowded situation as four ligands have to be accommodated. However, the T_m values of duplex **31**·**12** indicate that the steric demanding AZT ligands are reasonably arranged protruding into the major groove without disturbing the DNA helix.

3. Conclusion

The 7-tripropargylamine-8-aza-7-deaza-2′-deoxyribonucleoside (**1**) was synthesized, converted into the phosphoramidite building block **10** and employed in solid-phase synthesis. Oligonucleotides incorporating **1** were prepared. Single or multiple

incorporations of **1** in place of dG have a positive effect on duplex stability, which is in the range of the non-branched octa-1,7-diynylated nucleoside **2**. The Cu(I) assisted 'double click' functionalization of both terminal triple bonds by the *Huisgen–Meldal-Sharpless* cycloaddition was investigated. The efficacy and versatility of the 'double click' reaction with AZT (**3**), the non-polar benzyl azide (**4**), the lipophilic 11-azidoundecanol (**5**) as well as the hydrophilic PEG ligand **6** on monomer **1** as well as on oligonucleotide level were demonstrated. The functionalization was performed on single-stranded oligonucleotides in solution and on solid support. Consequently, nucleoside **1** is a versatile synthon being applicable for the construction of nucleolipids, or nucleoside–PEG or DNA–PEG conjugates, which are promising candidates for oligonucleotide drug or antisense delivery systems. The 'double click' chemistry on **1** allows the simultaneous functionalization of DNA with two reporter groups per single residue. Even in a steric crowded situation, when two modified residues of **1** are placed side by side within a single-stranded oligonucleotide, the 'double click' reaction proceeded smoothly. Hence, the tripropargylated nucleoside **1** can be considered as an 'ideal clickable' target for density functionalization of DNA even with bulky reporter groups being placed in a proximal position.

4. Experimental section

4.1. General

Monomers. All chemicals were purchased from Acros, Fluka, or Sigma–Aldrich (Sigma–Aldrich Chemie GmbH, Deisenhofen, Germany). Solvents were of laboratory grade. Thin layer chromatography (TLC): aluminum sheets, silica gel 60 F_{254} (0.2 mm; Merck, Darmstadt, Germany). Flash column chromatography (FC): silica gel 60H (VWR, Darmstadt, Germany) at 0.4 bar; sample collection with an Ultra Rac II fraction collector (LKB Instruments, Sweden). UV spectra: U-3200 spectrometer (Hitachi, Tokyo, Japan); λ_{max} in nm, ε in $dm^3\,mol^{-1}\,cm^{-1}$. Reversed-phase HPLC was carried out on a 250×4 mm RP-18 LiChrospher 100 column (Merck, Darmstadt, Germany) with a Merck–Hitachi HPLC pump connected with a variable wavelength monitor, a controller and an integrator. Gradients used for HPLC chromatography (A=MeCN, *B*=0.1 M (Et_3NH)OAc (pH 7.0)/MeCN, 95:5): (I): 3 min 15% A in B, 12 min 15–50% A in B, and 5 min 50–10% A in B, flow rate 0.7 mL/min; (II) 0–25 min 0–20% A in B, flow rate 0.7 mL/min; (III) 0–10 min 0–20% A in B, 10–15 min 20–40% A in B, 15–20 min 60% A in B, 20–25 min 40–0% A in B, flow rate 0.7 mL/min; (IV) 0–10 min 0–20% A in B, 10–30 min 20–30% A in B, 30–35 min 30–0% A in B, flow rate 0.7 mL/min. NMR spectra: Avance-DPX-300 spectrometer (Bruker, Rheinstetten, Germany), at 300.15 MHz for ^1H, 75.48 MHz for ^{13}C and 121.52 MHz for ^{31}P; δ in parts per million relative to Me_4Si as internal standard or 85% H_3PO_4 for ^{31}P. The *J* values are given in hertz. MALDI-TOF mass spectra were recorded with a Voyager-DE PRO spectrometer (Applied Biosystems) in the linear negative mode with 3-hydroxypicolinic acid (3-HPA) as a matrix. The detected masses were identical to the calculated values. Elemental analyses were performed by Mikroanalytisches Laboratorium Beller (Göttingen, Germany). The melting temperature curves were measured with a Cary-100 Bio UV–vis spectrophotometer (Varian, Australia) equipped with a Cary thermoelectrical controller. The temperature was measured continuously in the reference cell with a Pt-100 resistor with a heating rate of 1 °C min^{-1}.

Oligonucleotides. The syntheses of oligonucleotides was performed on a DNA synthesizer, model 392–08 (Applied Biosystems, Weiterstadt, Gemany) on a 1 μmol scale using the phosphoramidite **10** and the standard phosphoramidite building blocks following the synthesis protocol for 3′-*O*-(2-cyanoethyl)phosphoramidites.[48] After cleavage from the solid support, the oligonucleotides were deprotected in 25% aqueous ammonia solution for 12–16 h at 60 °C. The purification of the 'trityl-on' oligonucleotides was carried out on reversed-phase HPLC (Merck-Hitachi-HPLC); RP-18 column; gradient system (I). The purified 'trityl-on' oligonucleotides were treated with 2.5% $Cl_2CHCOOH/CH_2Cl_2$ for 5 min at 0 °C to remove the 4,4′-dimethoxytrityl residues. The detritylated oligomers were purified by reversed-phase HPLC (gradient II). The oligomers were desalted on a short column (RP-18, silica gel) using bidistilled water for elution of salt, while the oligomers were eluted with H_2O/MeOH (2:3). Then, they were lyophilized on a Speed-Vac evaporator to yield colorless solids, which were frozen at −24 °C. The molecular masses of the oligonucleotides were determined by MALDI-TOF mass spectrometry in the linear negative mode (see Table 7). Extinction coefficients ε_{260} of the nucleosides: dA 15 400, dG 11 700, dT 8 800, dC 7300, **1** 14 000, **21** 14 000, **22** 27 800, **23** 15 300 and **24** 14 600.

*4.1.1. 6-Amino-1-(2-deoxy-β-D-erythro-pentofuranosyl)-1,5-dihydro-{3-[di(prop-2-ynl)amino]prop-1-ynyl}-4H-pyrazolo[3,4-d]pyrimidin-4-one (**1**).* A solution of **7** (1.2 g, 3.0 mmol) in dry DMF (6 mL) was treated with CuI (80 mg, 0.4 mmol), $[Pd^0[P(Ph_3)_4]$ (178 mg, 0.15 mmol), anhydrous Et_3N (0.6 mL, 0.3 mmol), and 10 equiv of tri(prop-2-ynyl)amine (3.9 g, 30 mmol). The reaction mixture was stirred under N_2 for 12 h (TLC monitoring). Then, the mixture was diluted with $MeOH/CH_2Cl_2$ (1:1, 30 mL), and Dowex HCO_3^- (100±200 mesh; 1.8 g) was added. After stirring for 15 min, the evolution of gas ceased. Stirring was continued for another 30 min, the resin was filtered off and washed with $MeOH/CH_2Cl_2$ (1:1, 200 mL). The solutions of the filtrates were combined, evaporated and the oily residue was adsorbed on silica gel and loaded on the top of a column. FC (silica gel, column 15×3 cm, CH_2Cl_2/MeOH, 95:5→90:10→85:15) afforded one main zone. Evaporation of the solvent furnished **1** as a brown foam (850 mg, 71%). TLC (CH_2Cl_2/MeOH, 80:20): R_f 0.57. UV (MeOH): λ_{max} 243 (31 800), 280 (sh) (6 500). ^1H NMR (300 MHz, DMSO-d_6) δ: 2.11–2.19 (m, 1H, H_α–C(2′)); 2.61–2.70 (m, 1H, H_β–C(2′)); 3.25 (m, 2H, 2×H–C≡C); 3.44–3.48 (m, 6H, 3×NCH_2); 3.64 (m, 2H, 2×H–C(5′)); 3.76–3.77 (m, 1H, H–C(4′)); 4.36 (m, 1H, H–C(3′)); 4.73 (t, *J*=5.4 Hz, 1H, HO–C(5′)); 5.23 (d, *J*=3.9 Hz, 1H, HO–C(3′)); 6.28 ('t', *J*=6.2 Hz, 1H, H–C(1′)); 6.79 (br s, 2H, H_2N); 10.69 (s, 1H, HN). Anal. Calcd for $C_{19}H_{20}N_6O_4$ (396.40): C, 57.57; H, 5.09; N, 21.20. Found: C, 57.23; H, 5.28; N, 20.95.

*4.1.2. 6-[(2-Methylpropanoylamino)]-1-(2-deoxy-β-D-erythro-pentofuranosyl)-1,5-dihydro-{3-[di(prop-2-ynyl)amino]prop-1-ynyl}-4H-pyrazolo[3,4-d]pyrimidin-4-one (**8**).* Compound **1** (700 mg, 1.8 mmol) was dried by repeated co-evaporation with anhydrous pyridine (3×10 mL), then the solid was dissolved in DMF (7 mL) and 1,1,1,3,3,3-hexamethyldisilazane (3.5 mL) was added to the solution. The mixture was stirred for 3 h at rt, then pyridine (7 mL) and isobutyric anhydride (7 mL) were added and stirring was continued overnight at rt. To the solution, methanol (14 mL) was added and the mixture was stirred for another 3 h. The solvent was evaporated, and the remaining oily residue was applied to FC (silica gel, column 8×3 cm, CH_2Cl_2/MeOH, 95:5). Evaporation of the main zone afforded **8** as a colorless foam (695 mg, 84%). TLC (CH_2Cl_2/MeOH, 90:10): R_f 0.43. UV (MeOH): λ_{max} 243 (sh) (21 500), 251 (23 800), 273 (17 200). ^1H NMR (300 MHz, DMSO-d_6) δ: 1.13 (d, *J*=6.8 Hz, 6H, 2×(H_3C)$_2$CH–); 2.19–2.27 (m, 1H, H_α–C(2′)); 2.69–2.82 (m, 2H, H_β–C(2′), C*H*(CH_3)$_2$); 3.25 (m, 2H, 2×H–C≡C–); 3.45–3.51 (m, 6H, 3×NCH_2); 3.69 (s, 2H, H–C(5′)); 3.77–3.82 (m, 1H, H–C(4′)); 4.40–4.41 (m, 1H, H–C(3′)); 4.72 ('t', *J*=5.3 Hz, 1H, HO–C(5′)); 5.28 (d, *J*=3.3 Hz, 1H, HO–C(3′)); 6.38 ('t', *J*=6.3 Hz, 1H, H–C(1′)); 11.89 (br s, 2H, 2×HN). Anal. Calcd for $C_{23}H_{26}N_6O_5$ (466.49): C, 59.22; H, 5.62; N, 18.02. Found: C, 59.32; H, 5.71; N, 17.93.

*4.1.3. 6-[(2-Methylpropanoylamino)]-1-[2-deoxy-5-O-(4,4′-dimethoxytrityl)-β-D-erythro-pentofuranosyl]-1,5-dihydro-{3-[di(prop-2-ynyl)amino]prop-1-ynyl}-4H-pyrazolo[3,4-d]pyrimidin-4-one (**9**).* Compound

8 (500 mg, 1.1 mmol) was dried by repeated co-evaporation with anhydrous pyridine, and then dissolved in dry pyridine (10 mL) and stirred with 4,4′-dimethoxytrityl chloride (500 mg, 1.4 mmol) in the presence of *N*,*N*-diisopropylethylamine (290 μL, 1.8 mmol) at rt. After 3 h, the solution was poured into 5% aqueous $NaHCO_3$ (100 mL) and extracted with CH_2Cl_2 (2×80 mL). The combined organic layers were dried (Na_2SO_4), the solvent was evaporated and the remaining oily residue was co-evaporated with toluene (3×10 mL) to afford a foamy residue, which was applied to FC (silica gel, column 10×4 cm, CH_2Cl_2/acetone, 90:10). Evaporation of the main zone afforded **9** as colorless foam (707 mg, 86%). TLC (CH_2Cl_2/CH_3OH, 90:10): R_f 0.57. UV (MeOH): λ_{max} 235 (34 200), 250 (sh) (26 600), 274 (19 300). ^{1}H NMR (300 MHz, DMSO-d_6) δ: 1.13 (d, J=6.9 Hz, 6H, (H_3C)$_2$CH–); 2.24–2.32 (m, 1H, H_α–C(2′)); 2.74–2.83 (m, 2H, H_β–C(2′), C*H*(CH$_3$)$_2$); 2.97–3.07 (m, 2H, 2×H–C(5′)); 3.27 (s, 2H, H–C≡C–); 3.46 (s, 4H, NCH_2); 3.68 (s, 2H, NCH_2); 3.71 (s, 6H, 2×OCH_3); 3.90–3.91 (m, 1H, H–C(4′)); 4.46–4.49 (m, 1H, H–C(3′)); 5.33 (d, J=4.5 Hz, 1H, HO–C(3′)); 6.41 (‘t’, J=4.4 Hz, 1H, H–C(1′)); 6.75–6.80 (m, 4H, arom. H); 7.15–7.31 (m, 9H, arom. H); 11.90, 11.97 (2 br s, 2H, 2×HN). Anal. Calcd for $C_{44}H_{44}N_6O_7$ (768.86): C, 68.73; H, 5.77; N, 10.93. Found: C, 68.89; H, 5.95; N, 10.79.

*4.1.4. 6-[(2-Methylpropanoylamino)]-1-[2-deoxy-5-O-(4,4′-dimethoxytrityl)-β-D-erythro-pentofuranosyl]-1,5-dihydro-{3-[di(prop-2-ynl)amino]prop-1-ynyl}-4H-pyrazolo[3,4-d]pyrimidin-4-one-3′-[(2-cyanoethyl)-N,N-(diisopropyl)]phosphoramidite (**10**).* A solution of **9** (550 mg, 0.70 mmol) in anhydrous CH_2Cl_2 (9 mL) was treated with anhydrous (^{i}Pr)$_2$NEt (255 μL, 1.50 mmol) at rt. Then 2-cyanoethyl diisopropylphosphoramidochloridite (230 μl, 0.92 mmol) was added. After 30 min, the solution was washed with saturated $NaHCO_3$ and extracted with CH_2Cl_2 (2×100 mL). The combined organic layer was dried (Na_2SO_4) and the solvent was evaporated. FC (silica gel, column 8×3 cm, CH_2Cl_2/acetone, 95:5) afforded **10** as a colorless foam (564 mg, 83%). TLC (CH_2Cl_2/acetone, 95:5): R_f 0.38. ^{31}P NMR (121.5 MHz, $CDCl_3$) δ: 147.8, 147.9.

*4.1.5. 6-Amino-1-(2-deoxy-β-D-erythro-pentofuranosyl)-1,5-dihydro-3-[di(1′,2′,3′-triazol-1-methylbenzyl)propargylamino}-4H-pyrazolo[3,4-d]pyrimidin-4-one (**21**).* To a solution of **1** (79.2 mg, 0.2 mmol) and **4** (63.8 mg, 0.48 mmol) in THF, water and *tert*-butanol (v/v/v=3:1:1, 5 mL), sodium ascorbate (80 μL, 0.08 mmol) of a freshly prepared 1 M solution in water and copper(II) sulfate pentahydrate 7.5% in water (67 μL, 0.02 mmol) were added. The mixture was stirred vigorously in the dark at rt for 16 h. The solvent was evaporated, and the residue was applied to FC (silica gel, column 10×4 cm, eluted with CH_2Cl_2/MeOH, 80:20). The main zone afforded **21** as a colorless powder (104 mg, 78%). TLC (CH_2Cl_2/MeOH, 80:20): R_f 0.62. UV (MeOH): λ_{max} 243 (31 000), 285 (sh) (7 000). ^{1}H NMR (300 MHz, DMSO-d_6) δ: 2.12–2.20 (m, 1H, H_α–C(2′)); 2.64–2.73 (m, 1H, H_β–C(2′)); 3.37–3.53 (m, 4H, 2×H–C(5′), NCH_2); 3.77–3.82 (m, 5H, 2×NCH_2, H–C(4′)); 4.37 (m, 1H, H–C(3′)); 4.75 (‘t’, J=5.4 Hz, 1H, OH–C(5′)); 5.25 (d, J=4.2 Hz, 1H, HO–C(3′)); 5.58 (s, 4H, 2×NCH_2); 6.31 (‘t’, J=6.3 Hz, 1H, H–C(1′)); 6.83 (br s, 2H, H_2N); 7.28–7.38 (m, 10H, arom. H); 8.18 (s, 2H, 2×H5-triazole)); 10.73 (s, 1H, HN). Anal. Calcd for $C_{33}H_{34}N_{12}O_4$ (662.28): C, 59.81; H, 5.17; N, 25.36. Found: C, 59.69; H, 5.22; N, 25.41. *m*/*z* (ESI-TOF) calcd for $C_{33}H_{34}N_{12}O_4Na$ (M+Na$^+$): 685.28; found: 685.27.

*4.1.6. 6-Amino-1-(2-deoxy-β-D-erythro-pentofuranosyl)-1,5-dihydro-3-{di[1′,2′,3′-triazol-((1,2,3,4-tetrahydro-5-methyl-2,4-dioxopyrimidin-1H-1-yl)-furan-3-yl)]-propargylamino}-4H-pyrazolo[3,4-d]pyrimidin-4-one (**22**).* The same procedure as described for **21**, with **1** (134 mg, 0.34 mmol) and **3** (216 mg, 0.81 mmol) in water/THF (v/v=1:3, 12 mL), sodium ascorbate (270 μL, 0.27 mmol) of a freshly prepared 1 M solution in water and copper(II) sulfate pentahydrate 7.5% in water (230 μL, 0.0675 mmol). The mixture was stirred vigorously in the dark at rt for 12 h. The solvent was evaporated, and the residue was applied to FC (silica gel, column 10×4 cm, CH_2Cl_2/MeOH, 80:20). Evaporation of the main zone gave **22** as a white powder (168 mg, 54%). TLC (CH_2Cl_2/MeOH, 80:20): R_f 0.14. UV (MeOH): λ_{max} 244 (31 000), 260 (27 800). ^{1}H NMR (300 MHz, DMSO-d_6); nucleoside atom numbering for the AZT-derived moiety, i.e., double (″) and triple (‴) primed locants δ: 1.81 (s, 6H, 2×H_3C–C(5″)); 2.12–2.20 (m, 1H, H_α–C(2′)); 2.59–2.81 (m, 5H, H_β–C(2′), 2×H–C(2‴)); 3.50–3.52 (m, 2H, 2×H–C(5′)); 3.60–3.68 (m, 6H, NCH_2, 4×H–C(5‴)); 3.76–3.77 (m, 3H, H–C(4′), 2×H–C(4‴)); 3.87 (s, 4H, 2×NCH_2); 4.21–4.23 (m, 2H, 2×HO–C(5‴)); 4.34–4.39 (m, 1H, H–C(3′)); 4.74 (‘t’, J=5.9 Hz, 1H, HO–C(5′)); 5.24–5.34 (m, 3H, HO–C(3′), 2×H–C(3‴)); 6.30 (‘t’, J=6.8 Hz, 1H, H–C(1′)); 6.43 (‘t’, J=6.5 Hz, 1H, H–C(1‴)); 6.83 (br s, 2H, H_2N); 7.83 (s, 2H, 2×H–(C6″)); 8.31 (s, 2H, 2×H5-triazole); 10.71 (s, 1H, HN(5)); 11.35 (s, 2H, 2×HN(3″)). Anal. Calcd for $C_{39}H_{46}N_{16}O_{12}$ (930.88): C, 50.32; H, 4.98; N, 24.07. Found: C, 49.96; H, 4.65; N, 23.74.

*4.1.7. 6-Amino-1-(2-deoxy-β-D-erythro-pentofuranosyl)-1,5-dihydro-3-[di(1′,2′,3′-triazol-1-hydroxyundecyl)propargylamino]-4H-pyrazolo[3,4-d]pyrimidin-4-one (**23**).* The same procedure as described for **21**, with **1** (79.2 mg, 0.20 mmol) and **5** (85.2 mg, 0.40 mmol) in water/THF (v/v=1:3, 6 mL), using sodium ascorbate (200 μL, 0.20 mmol) of a freshly prepared 1 M solution in water and copper(II) sulfate pentahydrate 7.5% in water (170 μL, 0.05 mmol). The mixture was stirred vigorously in the dark at rt for 16 h. The solvent was evaporated, and the residue was applied to FC (silica gel, column 10×4 cm, eluted with CH_2Cl_2/MeOH, 80:20). Evaporation of the main zone gave **23** as a white powder (88 mg, 54%). TLC (silica gel, CH_2Cl_2/MeOH, 80:20): R_f 0.77. UV (MeOH): λ_{max} 243 (29 500), 286 (6 200). ^{1}H NMR (300 MHz, DMSO-d_6) δ: 1.20 (s, 32H, 16×CH_2); 1.35–1.37 (m, 4H, 2×CH_2); 1.78–1.82 (m, 4H, 2×CH_2); 2.12–2.19 (m, 1H, H_α–C(2′)); 2.64–2.72 (m, 1H, H_β–C(2′)); 3.40–3.50 (m, 4H, 2×H–C(5′), NCH_2); 3.77–3.80 (m, 5H, 2×NCH_2, H–(C4′)); 4.30–4.34 (m, 7H, H–C(3′), 2×*H*O–CH_2–, 2×–CH_2–); 4.73–4.77 (t, J=5.1 Hz, 1H, HO–C(5′)); 5.24–5.25 (d, J=4.2 Hz, 1H, HO–C(3′)); 6.28–6.32 (‘t’, J=6.3 Hz, 1H, H–C(1′)); 6.81 (br s, 2H, H_2N); 8.13 (s, 2H, 2×H5-triazole); 10.73 (s, 1H, HN). Anal. Calcd for $C_{41}H_{66}N_{12}O_6$ (823.04): C, 59.83; H, 8.08; N, 20.42. Found: C, 59.95; H, 8.01; N, 20.35.

*4.1.8. 6-Amino-1-(2-deoxy-β-D-erythro-pentofuranosyl)-1,5-dihydro-3-{di[1′,2′,3′-triazol-(tetra-ethoxy-methyl)]propargylamino}-4H-pyrazolo[3,4-d]]pyrmidin-4-one (**24**).* The same procedure as described for **21**, with **1** (79.2 mg, 0.20 mmol) and **6** (93.3 mg, 0.40 mmol) in water/THF (v/v=1:3, 6 mL), using sodium ascorbate (200 μL, 0.20 mmol) of a freshly prepared 1 M solution in water and copper(II) sulfate pentahydrate 7.5% in water (170 μL, 0.05 mmol). The mixture was stirred vigorously in the dark at rt for 16 h. The solvent was evaporated, and the residue was applied to FC (silica gel, column 10×4 cm, eluted with CH_2Cl_2/MeOH, 80:20). Evaporation of the main zone gave **24** as a yellow gum (67 mg, 39%). TLC (silica gel, CH_2Cl_2/MeOH, 80:20): R_f 0.67. UV (MeOH): λ_{max} 243 (26 800), 286 (sh) (6 700). ^{1}H NMR (300 MHz, DMSO-d_6) δ: 2.12–2.19 (m, 1H, H_α–C(2′)); 2.64–2.72 (m, 1H, H_β–C(2′)); 3.21 (s, 6H, 2×CH_3); 3.37–3.51 (m, 28H, 2×H–C(5′), NCH_2, 12×CH_2); 3.77–3.82 (m, 9H, 2×CH_2, 2×NCH_2, H–C(4′)); 4.36 (m, 1H, H–C(3′)); 4.52 (t, J=4.5 Hz, 4H, 2×CH_2); 4.74 (t, J=5.1 Hz, 1H, HO–C(5′)); 5.24 (d, J=3.9 Hz, 1H, HO–C(3′)); 6.30 (‘t’, J=6.0 Hz, 1H, H–C(1′)); 6.81 (br s, 2H, H_2N); 8.09 (s, 2H, 2×H5-triazole); 10.74 (s, 1H, HN). Anal. Calcd for $C_{37}H_{58}N_{12}O_{12}$ (862.93): C, 51.50; H, 6.77. Found: C, 51.69; H, 6.58.

*4.1.9. ‘Double click’ reaction performed in aqueous solution. Procedure for oligonucleotides **13**, **14** containing one modification site and the azides **3** or **4**.* To the single-stranded oligonucleotide **13** or **14** (5.0 A_{260} units) in H_2O (10–20 μL), a mixture of a $CuSO_4$–TBTA (1:1) ligand complex (premixed from 50 μL of a 20 mM stock solution in H_2O/DMSO/*t*-BuOH, 4:3:1 for TBTA and 50 μL of a 20 mM

stock solution in H_2O/DMSO/*t*-BuOH, 4:3:1 for $CuSO_4$) was added. Then, tris(carboxyethyl)phosphine (TCEP; 50 μL of a 20 mM stock solution in water), the corresponding azide **3** or **4** (50 μL of a 20 mM stock solution in dioxane/H_2O, 1:1), sodium bicarbonate (50 μL of a 200 mM aqueous solution) and 30 μL of DMSO were added, and the reaction mixture was stirred at rt for 12 h. The reaction mixture was concentrated in a Speed-Vac evaporator and dissolved in 1 mL of bidistilled water and centrifuged for 20 min at 12,000 rpm. The supernatant solution was decanted and oligonucleotides **25**, **26** and **29**, **30** were purified by reversed-phase HPLC with the gradient (III) for **25** and **26** and the gradient (IV) for **29** and **30**. The resulting oligonucleotides **25**, **26** and **29**, **30** were desalted on a RP-18 column and analyzed by HPLC RP-18 chromatography (see Supplementary data, Figs. S4 and S5) and MALDI-TOF mass spectrometry in the negative linear mode (Table 7).

*4.1.10. 'Double click' reaction performed in aqueous solution. Procedure for oligonucleotides **13**, **14** containing one modification site and the azides **5** or **6**.* As described for the azides **3** and **4**, with the single-stranded oligonucleotide **13** or **14** (3.0 A_{260} units) in H_2O (10–20 μL), a mixture of a $CuSO_4$–TBTA (1:1) ligand complex (premixed from 30 μL of a 20 mM stock solution in H_2O/DMSO/*t*-BuOH, 4:3:1 for TBTA and 30 μL of a 20 mM stock solution in H_2O/DMSO/*t*-BuOH, 4:3:1 for $CuSO_4$), tris(carboxyethyl)phosphine (TCEP; 30 μL of a 20 mM stock solution in water), the corresponding azide **5** or **6** (60 μL of a 20 mM stock solution in dioxane/H_2O, 1:1), sodium bicarbonate (30 μL of a 200 mM aqueous solution) and 30 μL of DMSO. The supernatant solution was decanted and purified by reversed-phase HPLC with the gradient (III). The resulting oligonucleotides **33**–**36** were analyzed by HPLC chromatography RP-18 (see Supplementary data, Fig. S6) and MALDI-TOF mass spectrometry in the negative linear mode (Table 7).

*4.1.11. 'Double click' reaction performed in aqueous solution. Procedure for oligonucleotides **15**, **16** containing two modification sites and the azides **3** or **4**.* As described for oligonucleotides containing one modified residue, with the single-stranded oligonucleotide **15** or **16** (5.0 A_{260} units) in H_2O (10–20 μL), a mixture of a $CuSO_4$-TBTA (1:1) ligand complex (premixed from 80 μL of a 20 mM stock solution in H_2O/DMSO/*t*-BuOH, 4:3:1 for TBTA and 80 μL of a 20 mM stock solution in H_2O/DMSO/*t*-BuOH, 4:3:1 for $CuSO_4$), tris(carboxyethyl)phosphine (TCEP; 80 μL of a 20 mM stock solution in water), the corresponding azide **3** or **4** (80 μL of a 20 mM stock solution in dioxane/H_2O, 1:1), sodium bicarbonate (80 μL of a 200 mM aqueous solution) and 50 μL of DMSO. The supernatant solution was decanted and purified by reversed-phase HPLC with the gradient (III) for **27** and **28** and the gradient (IV) for **31** and **32**. The resulting oligonucleotides **27**, **28** and **31**, **32** were desalted on a RP-18 column and analyzed by HPLC RP-18 chromatography (see Supplementary data, Figs. S4 and S5) and MALDI-TOF mass spectrometry in the negative linear mode (Table 7).

*4.1.12. 'Double click' reaction performed on solid support. Procedure for oligonucleotide **37** containing one modification site and the azides **3** or **4**. General procedure.* The single-stranded oligonucleotide **37** attached to a solid support (19 mg, 32 μmol/g, loading 500 Å) bearing the $(MeO)_2$Tr-protected residue as well as the nucleobases adenine and cytosine with *t*BPA (4-*tert*-butylphenoxy)acetyl protection and guanine with isobutyryl (iB) protecting groups was suspended in an aqueous solution of a $CuSO_4$ · TBTA ligand complex (300 μL; premixed from 150 μL of a 20 mM stock soln of $CuSO_4$ in H_2O/DMSO/*t*-BuOH, 4:3:1 and 150 μL of a 20 mM stock soln of TBTA in H_2O/DMSO/*t*-BuOH, 4:3:1). To this were added tris(carboxyethyl)phosphine (TCEP; 180 μL of a 20 mM stock soln in H_2O), AZT (**3**) (250 μL of a 20 mM stock soln in dioxane/H_2O, 1:1) or benzyl azide (**4**) (100 μL of a 200 mM stock soln in dioxane/H_2O, 1:1), $NaHCO_3$ (90 μL of a 200 mM stock soln in H_2O), DMSO (180 μL), and the mixture was stirred at rt for 2 days and then concentrated. The crude modified CPG-bound **38** and **39** were washed with H_2O/MeOH (4 mL, 1:1, v/v), followed by treatment with aqueous NH_3 solution (25%) for 14 h at 60 °C. During this procedure, the oligonucleotides attached to the solid support as well as the protecting groups of the nucleobases were removed. The 'trityl-on' oligonucleotides **40** and **41** were purified by reversed-phase HPLC (gradient I). The detritylated oligonucleotides were further purified by reversed-phase HPLC and desalted on a RP-18 column to give oligonucleotides **29** (gradient IV) and **25** (gradient III). The functionalized oligonucleotides **29** and **25** were analyzed by HPLC RP-18 chromatography (see Supplementary data) and MALDI-TOF mass spectrometry in the negative linear mode; **29**: $[M-1]^-$, calcd 4307.0; found: 4306.5 and **25**: $[M-1]^-$, calcd 4038.9; found: 4038.7.

*4.1.13. 'Double click' reaction performed on solid support. Procedure for oligonucleotide **42** containing two modification sites and the azides **3** or **4**. General procedure.* As described for oligonucleotide **37** with the single-stranded oligonucleotide **42** attached to a solid support (21 mg, 32 μmol/g, loading 500 Å), an aqueous solution of a $CuSO_4$ · TBTA ligand complex (600 μL; premixed from 300 μL of a 20 mM stock soln of $CuSO_4$ in H_2O/DMSO/*t*-BuOH, 4:3:1 and 300 μL of a 20 mM stock soln of TBTA in H_2O/DMSO/*t*-BuOH, 4:3:1), tris(carboxyethyl)phosphine (TCEP; 360 μL of a 20 mM stock soln in H_2O), AZT (**3**) (480 μL of a 20 mM stock soln in dioxane/H_2O, 1:1) or benzyl azide (**4**) (180 μL of a 200 mM stock soln in dioxane/H_2O, 1:1), $NaHCO_3$ (180 μL of a 200 mM stock soln in H_2O), DMSO (300 μL), at rt for 2 days and then concentrated. The crude modified CPG-bound **43** and **44** were washed with H_2O/MeOH (4 mL, 1:1, v/v), followed by treatment with aqueous NH_3 solution (25%) for 14 h at 60 °C. The 'trityl-on' oligonucleotides **45** and **46** were purified by reversed-phase HPLC as described above to give oligonucleotides **32** (gradient IV) and **28** (gradient III). The functionalized oligonucleotides **32** and **28** were analyzed by HPLC RP-18 chromatography (see Supplementary data) and MALDI-TOF mass spectrometry in the negative linear mode; **32**: $[M-1]^-$, calcd 4970.7; found: 4970.9 and **28**: $[M-1]^-$, calcd 4434.3; found: 4433.8.

Acknowledgements

We thank Mr. N.Q. Tran for the oligonucleotide synthesis, and Dr. R. Thiele from Roche Diagnostics, Penzberg, Germany, for the measurement of the MALDI spectra. We thank Dr. P. Leonard for his continuous support throughout the preparation of the manuscript and appreciate critical reading of the manuscript by Mr. S. Pujari. Financial support by the Roche Diagnostics GmbH and Chem-Biotech, Münster, Germany, is gratefully acknowledged.

Supplementary data

pK_a determination of 7-tripropargylamino-8-aza-7-deaza-2′-deoxyguanosine (**1**) by UV spectroscopy. HPLC profile of AZT (**3**) and 'double click' conjugate **32**. HPLC profiles of modified oligonucleotides (**14**–**16**, **19**, **20**). HPLC profiles of 'double click' oligonucleotide conjugates (**25**–**33**, **35**). ^{1}H NMR and ^{13}C NMR spectra of new compounds (Figs. S7–S21); and ^{31}P NMR spectrum of phosphoramidite **10** (Fig. S13). Supplementary data associated with this article can be found in online version, at doi:10.1016/j.tet.2010.03.086.

References and notes

1. Meldal, M.; Tornøe, C. W. *Chem. Rev.* **2008**, *108*, 2952.
2. Kolb, H. C.; Finn, M. G.; Sharpless, K. B. *Angew. Chem., Int. Ed.* **2001**, *40*, 2004.
3. Moses, J. E.; Moorhouse, A. D. *Chem. Soc. Rev.* **2007**, *36*, 1249.
4. Jewett, J. C.; Bertozzi, C. R. *Chem. Soc. Rev.* **2010**, *39*, 1272.

5. Wang, Q.; Chan, T. R.; Hilgraf, R.; Fokin, V. V.; Sharpless, K. B.; Finn, M. G. *J. Am. Chem. Soc.* **2003**, *125*, 3192.
6. Binder, W. H.; Kluger, C. *Curr. Org. Chem.* **2006**, *10*, 1791.
7. Nandivada, H.; Jiang, X.; Lahann, J. *Adv. Mater* **2007**, *19*, 2197.
8. Díaz, D. D.; Punna, S.; Holzer, P.; McPherson, A. K.; Sharpless, K. B.; Fokin, V. V.; Finn, M. G. *J. Polym. Sci., Part A: Polym. Chem.* **2004**, *42*, 4392.
9. Amblard, F.; Cho, J. H.; Schinazi, R. F. *Chem. Rev.* **2009**, *109*, 4207.
10. Kolb, H. C.; Sharpless, K. B. *Drug Discovery Today* **2003**, *8*, 1128.
11. Gramlich, P. M. E.; Wirges, C. T.; Gierlich, J.; Carell, T. *Org. Lett.* **2008**, *10*, 249.
12. Gogoi, K.; Mane, M. V.; Kunte, S. S.; Kumar, V. A. *Nucleic Acids Res.* **2007**, *35*, e139.
13. Chittepu, P.; Sirivolu, V. R.; Seela, F. *Bioorg. Med. Chem.* **2008**, *16*, 8427.
14. Jawalekar, A. M.; Meeuwenoord, N.; Cremers, J. G. O.; Overkleeft, H. S.; van der Marel, G. A.; Rutjes, F. P. J. T.; van Delft, F. L. *J. Org. Chem.* **2008**, *73*, 287.
15. Pourceau, G.; Meyer, A.; Vasseur, J.-J.; Morvan, F. *J. Org. Chem.* **2009**, *74*, 1218.
16. Bouillon, C.; Meyer, A.; Vidal, S.; Jochum, A.; Chevolot, Y.; Cloarec, J.-P.; Praly, J.-P.; Vasseur, J.-J.; Morvan, F. *J. Org. Chem.* **2006**, *71*, 4700.
17. Alvira, M.; Eritja, R. *Chem. Biodiv.* **2007**, *4*, 2798.
18. Lönnberg, H. *Bioconjugate Chem.* **2009**, *20*, 1065.
19. Devaraj, N. K.; Miller, G. P.; Ebina, W.; Kakaradov, B.; Collman, J. P.; Kool, E. T.; Chidsey, C. E. D. *J. Am. Chem. Soc.* **2005**, *127*, 8600.
20. (a) Seela, F.; Sirivolu, V. R. *Chem. Biodiv.* **2006**, *3*, 509; (b) Seela, F.; Sirivolu, V. R. *Helv. Chim. Acta* **2007**, *90*, 535.
21. Seo, T. S.; Bai, X.; Ruparel, H.; Li, Z.; Turro, N. J.; Ju, J. *Proc. Natl. Acad. Sci. U.S.A.* **2004**, *101*, 5488.
22. Chevolot, Y.; Bouillon, C.; Vidal, S.; Morvan, F.; Meyer, A.; Cloarec, J.-P.; Jochum, A.; Praly, J.-P.; Vasseur, J.-J.; Souteyrand, E. *Angew. Chem., Int. Ed.* **2007**, *46*, 2398.
23. Collman, J. P.; Devaraj, N. K.; Chidsey, C. E. D. *Langmuir* **2004**, *20*, 1051.
24. Gramlich, P. M. E.; Wirges, C. T.; Manetto, A.; Carell, T. *Angew. Chem., Int. Ed.* **2008**, *47*, 8350.
25. Seela, F.; Sirivolu, V. R.; Chittepu, P. *Bioconjugate Chem.* **2008**, *19*, 211.
26. Seela, F.; Ming, X. *Helv. Chim. Acta* **2008**, *91*, 1181.
27. Seela, F.; Xiong, H.; Leonard, P.; Budow, S. *Org. Biomol. Chem.* **2009**, *7*, 1374.
28. Seela, F.; Sirivolu, V. R. *Org. Biomol. Chem.* **2008**, *6*, 1674.
29. Gierlich, J.; Burley, G. A.; Gramlich, P. M. E.; Hammond, D. M.; Carell, T. *Org. Lett.* **2006**, *8*, 3639.
30. Sirivolu, V. R.; Chittepu, P.; Seela, F. *ChemBioChem* **2008**, *9*, 2305.
31. Gramlich, P. M. E.; Warncke, S.; Gierlich, J.; Carell, T. *Angew. Chem., Int. Ed.* **2008**, *47*, 3442.
32. Seela, F.; Ingale, S. A. *J. Org. Chem.* **2010**, *75*, 284.
33. (a) Seela, F.; Peng, X.; Budow, S. *Curr. Org. Chem.* **2007**, *11*, 427; (b) Seela, F.; Shaikh, K. I. *Tetrahedron* **2005**, *61*, 2675.
34. Rosemeyer, H. *Chem. Biodiv.* **2005**, *2*, 977.
35. Ahlers, M.; Ringsdorf, H.; Rosemeyer, H.; Seela, F. *Colloid Polym. Sci.* **1990**, *268*, 132.
36. Banchelli, M.; Berti, D.; Baglioni, P. *Angew. Chem., Int. Ed.* **2007**, *46*, 3070.
37. Jeong, J. H.; Kim, S. W.; Park, T. G. *Bioconjugate Chem.* **2003**, *14*, 473.
38. Berndl, S.; Herzig, N.; Kele, P.; Lachmann, D.; Li, X.; Wolfbeis, O. S.; Wagenknecht, H.-A. *Bioconjugate Chem.* **2009**, *20*, 558.
39. Weisbrod, S. H.; Marx, A. *Chem. Commun.* **2008**, 5675.
40. Gierlich, J.; Gutsmiedl, K.; Gramlich, P. M. E.; Schmidt, A.; Burley, G. A.; Carell, T. *Chem.—Eur. J.* **2007**, *13*, 9486.
41. (a) Seela, F.; He, Y.; He, J.; Becher, G.; Kröschel, R.; Zulauf, M.; Leonard, P. In *Methods in Molecular Biology*; Herdewijn, P., Ed.; Humana: Totowa, NJ, 2004; Vol. 288, pp 165–186; (b) Seela, F.; Becher, G. *Synthesis* **1998**, 207; (c) Seela, F.; Becher, G. *Chem. Commun.* **1998**, 2017.
42. Shen, R.; Huang, X. *Org. Lett.* **2008**, *10*, 3283.
43. Seela, F.; Steker, H. *Helv. Chim. Acta* **1986**, *69*, 1602.
44. Thibaudeau, C.; Plavec, J.; Chattopadhyaya, J. *J. Org. Chem.* **1996**, *61*, 266.
45. Blackburn, G. M.; Gait, M. J. *Nucleic Acids in Chemistry and Biology*; Oxford University Press: Oxford, 1996; p 18.
46. Smrt, J.; Hynie, S. *Collect. Czech. Chem. Commun.* **1980**, *45*, 927.
47. Luisi, P. L. *Anat. Rec.* **2002**, *268*, 208.
48. User's Manual of the DNA Synthesizer, Applied Biosystems, Weiterstadt, Germany.